

Attributing a Causal Agent and Assessing the Severity of Non-Stand Replacing Disturbances in a Northern Hardwood Forest using Landsat-Derived Vegetation Indices

Alexandre Morin-Bernard, Alexis Achim & Nicholas C. Coops

To cite this article: Alexandre Morin-Bernard, Alexis Achim & Nicholas C. Coops (2023) Attributing a Causal Agent and Assessing the Severity of Non-Stand Replacing Disturbances in a Northern Hardwood Forest using Landsat-Derived Vegetation Indices, Canadian Journal of Remote Sensing, 49:1, 2196356, DOI: [10.1080/07038992.2023.2196356](https://doi.org/10.1080/07038992.2023.2196356)

To link to this article: <https://doi.org/10.1080/07038992.2023.2196356>



© 2023 The Author(s). Published by Informa UK Limited, trading as Taylor & Francis Group.



Published online: 10 Apr 2023.



Submit your article to this journal [↗](#)



Article views: 2851



View related articles [↗](#)



View Crossmark data [↗](#)

Attributing a Causal Agent and Assessing the Severity of Non-Stand Replacing Disturbances in a Northern Hardwood Forest using Landsat-Derived Vegetation Indices

Attribution d'un agent causal et mesure de la sévérité de perturbations intermédiaires en forêt feuillue nordique à partir d'indices de végétation dérivés de Landsat

Alexandre Morin-Bernard^a, Alexis Achim^a , and Nicholas C. Coops^b 

^aDepartment of Wood and Forest Sciences, Université Laval, 2425 rue de la Terrasse, Québec, QC, G1V 0A6, Canada; ^bDepartment of Forest Resources Management, University of British Columbia, 2424 Main Mall, Vancouver, BC, V6T 1Z4, Canada

ABSTRACT

Non-stand-replacing disturbances are major drivers of northern hardwood forest dynamics, but are more challenging to characterize using satellite imagery than stand-replacing events. This study proposes a hurdle approach in which disturbance causal agents are first attributed to permanent sample plots that were either partially harvested, had sustained damage from an ice storm or remained undisturbed during the observation period, reaching an overall accuracy of 82.9%. Ordinary least square regression was then used to develop disturbance-specific models to assess the severity of partial harvests and damage from ice storms, with r -squared values of 0.57 and 0.59, respectively. The disturbance-specific models included a different set of predictors, confirming the importance of attributing a causal agent to a disturbance before assessing its severity. The sequence of models was implemented regionally to produce severity maps for two disturbance events, revealing within-stand variability in the severity that could be useful for the planning of future silvicultural actions. Although the proposed models offer acceptable performance, more research is needed to include additional disturbance agents and develop models that better capture the small variations in the spectral reflectance caused by low-severity disturbances, especially in the case of low-intensity partial harvests.

RÉSUMÉ

Les perturbations intermédiaires influencent fortement la dynamique des forêts de feuillues nordiques, mais sont plus difficiles à détecter et à caractériser à l'aide de l'imagerie satellitaire que les perturbations de forte intensité. Cette étude propose une approche par étapes dans laquelle les agents causaux des perturbations sont d'abord attribués à des placettes-échantillon permanentes qui ont été partiellement récoltées, ont subi des dommages dus au verglas ou sont restées intactes pendant la période d'observation avec une précision globale de 82.9%. Des modèles linéaires distincts permettant l'estimation de la sévérité des coupes partielles et des dommages dus au verglas ont ensuite été développés, dont les coefficients de détermination respectifs sont de 0.57 et 0.59. Les modèles spécifiques aux perturbations comprenaient un ensemble différent de prédicteurs, confirmant l'importance d'attribuer un agent causal à une perturbation avant d'en évaluer la sévérité. Les modèles ont été appliqués régionalement pour estimer la sévérité de deux événements ponctuels, révélant une variabilité dans la sévérité à une échelle inférieure à celle du peuplement forestier. Cette information pourrait permettre une meilleure planification des actions sylvicoles futures. Bien que les modèles proposés offrent une performance satisfaisante, des recherches supplémentaires sont nécessaires pour inclure davantage de types de perturbations intermédiaires et pour développer des modèles qui capturent mieux les variations subtiles de la sévérité des perturbations intermédiaires, en particulier dans le cas des coupes partielles de faible intensité.

ARTICLE HISTORY

Received 14 November 2022
Accepted 23 March 2023

Introduction

Northern hardwood forests are among the most complex and biologically diverse ecosystems in Canada, providing some of its most valued wood products. Their dynamics are driven by disturbances caused by biotic and abiotic agents such as wind, freezing rain, pathogens and herbivory insects, resulting in canopy gaps of varying extent and a characteristic uneven-aged structure. The return interval of such non-stand-replacing disturbances in these forests is much shorter than that of severe, stand-replacing disturbances, which can reach thousands of years (Payette et al. 1990; Seymour et al. 2002). Although the impact of an individual disturbance is limited, the composite effect of these low- to moderate severity events at the ecosystem scale is a key driver of forest composition, structure and biomass dynamics (Payette et al. 1990; Woods 2000; Woods and Kern 2022). Northern hardwood forests are also subject to anthropogenic disturbances such as harvesting, which become the main driver of forest compositional changes in the most intensively managed regions (Danneyrolles et al. 2019).

Silvicultural systems in these forests generally rely on partial harvesting (Figure 1(a)), which involves removing between 15% and 50% of the basal area (BA, $\text{m}^2 \cdot \text{ha}^{-1}$) of a stand i.e., the sum of the cross-sectional areas of tree stems at 1.3 m in height over a unit area of land (Merrill 1935). The use of BA in silvicultural prescriptions has the dual advantage of avoiding the imprecision of volume estimates due to the complex architecture of broadleaved trees and being linked to the understory light regime within a stand. Manipulation of BA through partial harvesting helps maintain the uneven-aged structure of forest stands over time by replicating the natural disturbance regime of northern hardwood forests characterized by the dominance of non-stand replacing disturbances (Leak et al. 2014; Seymour et al. 2002). Such silvicultural systems, therefore, favor the regeneration of species with intermediate to high tolerance to shade (Grayson et al. 2012; Jenkins and Chambers 1989).

The projected increase in the frequency and severity of extreme climate events (Peng et al. 2011; Seidl et al. 2017) will inevitably affect the way northern hardwood forests are shaped by disturbances. The

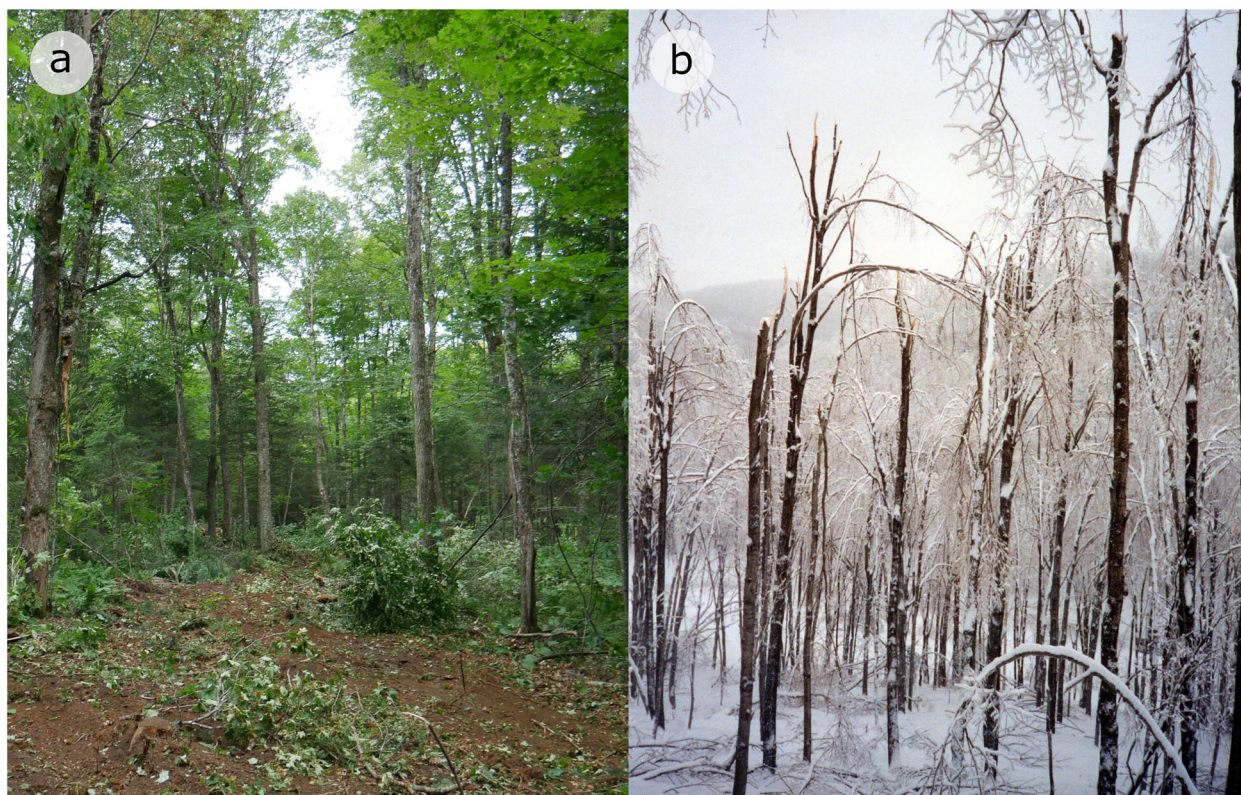


Figure 1. (a) Hardwood stand with soil exposed in the logging trails after a partial harvest. (b) Hardwood stands in which crowns were severely damaged consecutively by an ice storm.

extent to which these changes will alter the ecosystem services they provide and their contribution to timber supply remains largely unknown (Gardiner and Moore 2014; Thom and Seidl 2016; Turner 2010). To better forecast these impacts and identify potential remedial actions, it is imperative to get a more accurate picture of the frequency, severity and extent of these more subtle disturbance events. This is usually not achievable from traditional forest inventory approaches, which rely on a limited number of ground plots that are not measured every year and that are not necessarily distributed representatively across the ecosystem (Bowman et al. 2013; Gillis et al. 2005).

Remote sensing from satellite imagery has become an indispensable tool to detect and characterize forest disturbances. Among available products, imagery from the Landsat program is now widely used for the monitoring of forest dynamics, providing continuous data since 1972 with a spatial resolution offering the possibility to study forest change both at global and regional scales, on short and long timescales (Banskota et al. 2014; Coppin and Bauer 1996; Wulder et al. 2022). The validity of conclusions drawn from such studies relies on the accuracy of the methods used to measure change. Detecting and assessing the severity of non-stand-replacing disturbances is much more challenging than it is for severe, stand-replacing disturbances, mostly because the changes they cause are of lower magnitude (Ahmed et al. 2017; Coops et al. 2020; Hermosilla et al. 2015a).

In broadleaved forests, Landsat has proven useful for studying non-stand replacing disturbances such as ice storms and partial harvests. Ice storms are severe events of freezing rain, causing the accumulation of heavy loads of ice on tree branches (Proulx and Greene 2001; Rhoads et al. 2002). This disturbance is common in eastern North America, where climate and physiography favor the development of the required combination of air and precipitation temperatures (Bennett 1959). In the region of Canada dominated by the northern hardwood forest ecosystem, ice accumulation from freezing rain occurs on an annual basis, influencing stand dynamics by causing variable levels of damage to tree crowns (Figure 1(a)), and causing mortality in moderately rare events where ice accumulation exceeds critical levels (Proulx and Greene 2001). In Eastern Ontario, Olthof et al. (2004) used measurements of damage to the canopy taken in 104 ground plots and concluded that changes in the Landsat-derived normalized difference vegetation index (NDVI) could not discriminate between many levels of damage, but could be useful to classify it in a

limited number of categories. In the same region and for the same ice storm event, King et al. (2005) used a combination of pre- and post-disturbance values of the Landsat blue, red and shortwave infrared bands as well as biophysical variables to model canopy loss as a continuous variable with moderate success. In the White Mountains in the north-eastern United States, Burnett (2002) classified damage after an ice storm measured in 288 sites in three categories using NDVI and a ratio of shortwave and near-infrared Landsat bands, with accuracy from 78% to 82%. In the Adirondack forests of New York, Millward and Kraft (2004) found a significant and linear relationship between the change in NDVI values and in-situ measurements of damage to the canopy taken on a limited number of plots (16) after an ice storm. In the Appalachian mountains, Stueve et al. (2007) also found a statistically significant, but the nonlinear relationship between NDVI changes and the number of downed trees after an ice storm.

Partial harvesting has also been studied using Landsat data. Franklin et al. (2000) concluded that Landsat indices derived from the Tasseled Cap transformation, combining the information contained in six Landsat bands through orthogonal transformation (Crist and Cicone 1984), were moderately accurate for the detection of partial harvests in New Brunswick, while NDVI was easily confused in hardwoods because of the lush understory. In a subsequent study, Franklin et al. (2001) used the Tasseled Cap Wetness (TCW) to classify harvested stands into three categories of intensity. In Maine, Wilson and Sader (2002), Sader et al. (2003) and Jin and Sader (2005) used the normalized difference moisture index (NDMI), based on one of the Landsat shortwave infrared bands in addition to the near-infrared band, to detect and classify clearcut and partial harvests. They concluded that this index performed better than NDVI, and similarly to TCW in detecting harvests. When comparing different harvest practices in British Columbia, Jarron et al. (2017) found that the magnitude of change in the normalized burn ratio (NBR) consecutively to harvesting was representative of the intensity of the studied harvest practices. The NBR was also used by Tortini et al. (2019) to map partial harvests and clearcut in Michigan. Although the detection of partial harvests has received considerable attention, measuring the intensity of the cut has received considerably less attention. Yet, a more precise estimation of the change in harvested stands would be useful for forest managers because the actual

basal area removal influences the post-harvest dynamics of the stand (Leak et al. 2014).

One of the main obstacles in studies dedicated to non-stand replacing disturbances is the availability of accurate data on the actual severity of the disturbances. Calibration and validation data are therefore frequently derived from indirect sources such as aerial surveys, high-resolution photos or other remote sensing products (e.g., Tortini et al. 2019). While such sources provide useful estimates of the extent of the damage over a large spatial coverage, they often comprise estimation errors that can limit the possibility to conduct analyses at a resolution that is useful for forest management (Johnson and Ross 2008). Field inventories provide the most accurate validation data but are uncommon because of the prohibitive collection costs and the need for measurements both before and after the disturbance. Yet, when available, such field-validated data allows a clear confirmation of the agent responsible for the disturbance and a precise quantification of the impacts of the disturbance on both the canopy and the sub-canopy layers (Rodman et al. 2021).

Studies on the detection and characterization of non-stand replacing disturbances using satellite imagery have resulted in approaches that rely on different Landsat bands and vegetation indices and have revealed distinct relationships between the change in spectral reflectance and the severity of the disturbances depending on the causal agent. An accurate assessment of the impacts of a disturbance, therefore, requires prior knowledge of its causal agent. Moreover, initial forest conditions are likely to influence the relationship between changes in spectral reflectance and the severity of the event (Harvey et al. 2019). Few studies have so far focused on classifying disturbances according to their causal agent, and those that did were either interested exclusively in stand-replacing disturbances (e.g., Coops et al. 2020), were classifying non-stand replacing disturbances versus stand-replacing disturbances (e.g., Hermosilla et al. 2015a), or were conducted in boreal forests in which the initial conditions tend to be more uniform (e.g., Ahmed et al. 2017).

The objective of this study was to identify Landsat-derived vegetation indices allowing the correct attribution of a causal agent to disturbances resulting from an ice storm and from partial harvests in northern hardwood forests. This study also aimed to identify indices that are appropriate to assess the severity of these disturbances. The influence of the pre-disturbance conditions of the stands on the relationships

between changes in surface reflectance and the severity of the disturbance was also investigated, and case studies were produced in which the severity of the two types of disturbance was mapped on samples of the study area.

Methods

Study area

The study area is located in southern Quebec, Canada, within woodlots owned by Domtar Corporation (Figure 2). Totalling more than 160 000 hectares, the forest estate stretches through two bioclimatic subdomains i.e., the American basswood (*Tilia americana* L.) and the sugar maple (*Acer saccharum* Marsh.)- yellow birch (*Betula alleghaniensis* Britt.) subdomains (Saucier et al. 2009). In the ecological districts where the woodlots are located, the mean annual temperature ranges from 2.5–5 °C and the growing season length varies between 160 and 190 days. These districts are characterized by mean annual precipitation between 1000 and 1100 mm (Gosselin 2005, 2007). Forests on mesic sites typically consist of uneven-aged stands, dominated by northern hardwood species, mainly sugar and red maples (*Acer rubrum* L.), yellow birch and American beech (*Fagus grandifolia* Ehrh.), with a smaller component of paper birch (*Betula papyrifera* Marsh.), white ash (*Fraxinus americana* L.), balsam fir (*Abies balsamea* [L.] Mill.) and red spruce (*Picea rubens* Sarg.). According to projections made using a thirteen global circulation model ensemble in climate NA (Wang et al. 2016), the maximum temperature in both summer and winter over the study area is expected to increase by 4.8 °C and 4.2 °C, respectively, based on an average of projections for shared socioeconomic pathways (SSP) 1–3 and 5 (Riahi et al. 2017).

Disturbance data

The forest inventory dataset used in this study comes from an extensive network of permanent sample plots established in hardwood-dominated stands between 1984 and 2010 and revisited periodically. Plots established from 1997 onwards are circular, with a radius of 11.28 m (400 m²) while plots established before 1997 had the same area but are rectangular. All trees with a diameter at breast height (DBH) greater than 90 mm were measured at each survey. Newly dead trees and newly recruited trees that had reached a DBH greater than 90 mm were also recorded at each visit. From all plots of the network, 140 were selected to be included

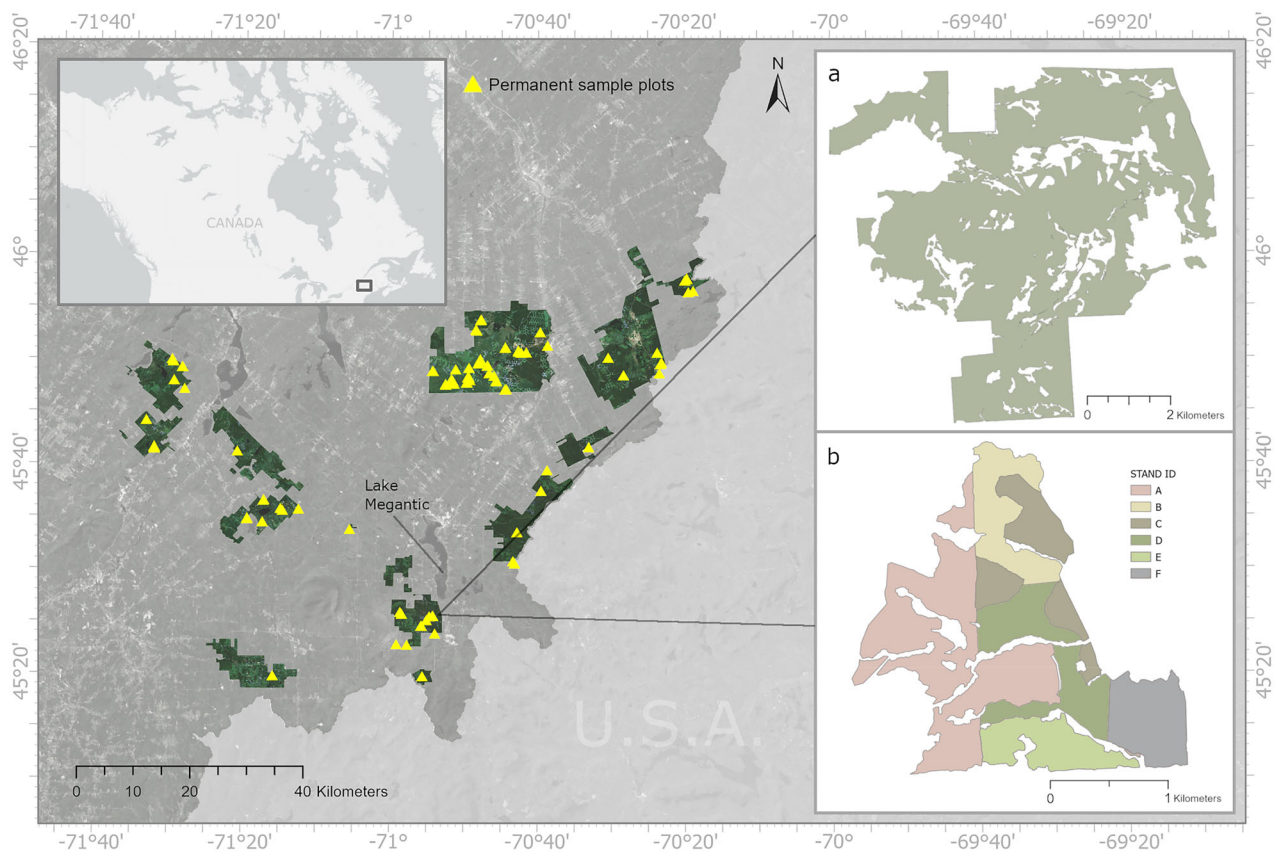


Figure 2. Location of the study area and of the two subsets used for model application. (a) Area of broadleaved-dominated stands on which the severity of the damage resulting from the ice storm was mapped. (b) Harvest area composed of six stands harvested in 2020 on which the basal area removal consecutively to the partial harvests was mapped.

in the current study. A partial harvest had occurred in 46 of these plots. Silvicultural treatments included shelterwood, selection and salvage cuts ranging from 16% to 50% of basal area removal, as assessed from the post-harvest field inventory. Partial harvest operations were conducted in these plots in one of fourteen years distributed in the period from 2001 to 2020. The exact dates were determined using the execution reports submitted after the operations. A minimum of one and a maximum of eight sample plots were harvested in each of the fourteen years of observation.

In addition, 47 plots that were damaged during a major ice storm event were selected. From 5 January 1998 to 9 January 1998, an unprecedented ice storm, depositing as much as 100 mm of ice in the worst affected areas, hit eastern Ontario, southern Quebec, and the northeast United States, causing devastation in the northern hardwood forests (Chabot et al. 1998; Irland 1998; Proulx and Greene 2001). Damage to crowns was assessed visually in the field during the growing season following the ice storm, by estimating the percentage of branches that were broken on each individual tree within the plot. The canopy damage at the plot level was obtained by averaging the damage

to the crowns of each tree, weighted by their respective basal area. The plot-averaged damage to the canopy ranged from 5% to 67%.

Finally, 47 control plots were randomly selected among the remaining plots of the network located in the same area, ensuring no disturbance was recorded in the surveys conducted before and after the assigned disturbance year. Fictive disturbance years were assigned to the control plots using a stratified approach creating a distribution of years similar to that of disturbed plots. A description of the pre-disturbance stand characteristics is presented in Table 1.

Development of the Landsat Surface Reflectance composites

Landsat TM, ETM+ and OLI Tier 1 Surface Reflectance scenes with less than 70% cloud cover, geometrically and atmospherically corrected, were used to create median composites for various years over each of the 140 selected plots. Only scenes acquired during the growing season in this region (i.e., June 1–August 30) were used. Pixels containing clouds or cloud shadows were masked and an additional

Table 1. Pre-disturbance characteristics of the plots included in the sample.

	Control	Harvest	Ice storm
Number of plots	47	46	47
Initial basal area ($\text{m}^2 \cdot \text{ha}^{-1}$)			
Average	22.7	26.0	25.7
Min	12.2	12.4	13.9
Max	39.2	39.7	39.0
Initial stem density ($\text{stem} \cdot \text{ha}^{-1}$)			
Average	552	572	617
Min	300	250	300
Max	1625	1150	1350
Mean DBH (cm)			
Average	23.6	24.9	24.0
Min	13.2	14.1	14.9
Max	34.7	33.9	33.5
Maples (% BA)			
Average	75.3	75.3	70.5
Min	7.1	31.8	15.7
Max	100	100	100
Yellow birch (% BA)			
Average	8.8	10.1	14.6
Min	0.0	0.0	0.0
Max	41.3	45.7	75.4
American beech (% BA)			
Average	5.0	9.9	9.7
Min	0.0	0.0	0.0
Max	42.9	67.1	46.3

Table 2. The number of scenes from each Landsat satellite used to build the composites.

Satellite	Number of scenes	First year	Last year
Landsat 5 TM	102	1996	2011
Landsat 7 ETM+	109	1999	2020
Landsat 8 OLI	35	2013	2021

visual inspection of the scenes was done to ensure the absence of undetected cloud shadows or thin clouds over the plots. A total of 246 scenes from Worldwide Reference System Paths 12 and 13, Rows 28 and 29 were used to create the composites, the acquisition dates ranging from 1996 to 2021 (Table 2).

A series of composite images were built separately for each plot, at different intervals depending on the date of the disturbance. Two distinct annual median composites were first produced for each plot from the scenes acquired in the two growing seasons preceding the disturbance. These composites were then averaged to produce a single pre-disturbance composite referred to as the reference composite. Scenes acquired in the growing season immediately following the disturbance were used to produce an additional composite, hereafter referred to as the disturbance composite. The ice storm, as well as most of the harvest operations, occurred between the second and third growing seasons because the harvest occurred in winter. For plots harvested during a growing season, scenes from the growing season corresponding to the harvest were attributed either to the reference or the disturbance composites depending on whether the image was

Table 3. The number of Landsat scenes used to build the composites for plots in each disturbance category and timing relative to the disturbance event.

Disturbance	Nbr of plots	Composites	Minimum	Maximum	Average
Control	47	Reference	1	14	6.1
		Disturbance	1	7	3.1
		Recovery	1	10	5.0
Harvest	46	Reference	2	18	7.7
		Disturbance	1	8	2.6
		Recovery	1	9	3.2
Ice storm	47	Reference	1	7	3.0
		Disturbance	1	6	2.4
		Recovery	3	15	7.6

captured before or after the date of harvest. A last composite was produced from the scenes acquired in the second growing season following the disturbance, which will be referred to as the post-disturbance composite. Between 1 and 18 scenes were used to build the reference, disturbance and post-disturbance composites depending on the plot and type of disturbance (Table 3). The Google Earth Engine platform (GEE, Gorelick et al. 2017) was used for scene extraction and compositing.

Calculation of vegetation indices and change metrics

Five vegetation indices were calculated from the median composites (Table 4). The NBR was originally developed to assess burn severity after wildfires (Key and Benson 2006), but has also proven useful to discriminate between different harvest intensities and detect a large variety of disturbances (Jarron et al. 2017; Kennedy et al. 2010). Two indices derived from the Tasseled Cap transformation, the TCW and TCA, were also included because of their known association with the density of the forest cover and their potential use in detecting forest removal and other disturbances (Franklin et al. 2000; Healey et al. 2006; Jin and Sader 2005). An index entirely based on the visible bands, the Green-Red Vegetation Index (GRVI) was also included in the study because of its sensitivity to phenology and subtle changes in the canopy of broadleaved forests (Motohka et al. 2010; Muraoka et al. 2013). The NDVI was also included as a reference, because of its extensive early studies on disturbance detection.

The average value of the vegetation indices was extracted from the composites over a 3×3 -pixel window enclosing the location of the plots, resulting in a short time series of three values per vegetation index per plot, representing the reference, disturbance and post-disturbance conditions, respectively. These values were used to compute two change metrics for each

Table 4. Vegetation indices, equations and references used in the current study.

Index	Equation	Reference
Normalized Difference Vegetation Index (NDVI)	$= (NIR - Red) / (NIR + Red)$	(Tucker 1979)
Normalized Burn Ratio (NBR)	$= (NIR - SWIR2) / (NIR + SWIR2)$	(Key and Benson 2006)
Green-Red Vegetation Index (GRVI)	$= (Green - Red) / (Green + Red)$	(Motohka et al. 2010; Tucker 1979)
Tasseled Cap Wetness (TCW)	$= 0.0315 * Blue + 0.2021 * Green + 0.3102 * Red + 0.1594 * NIR - 0.6806 * SWIR1 - 0.6109 * SWIR2$	(Crist 1985)
Tasseled Cap Angle (TCA)	$= \arctan(TCG/TCB)$ $TCG = -0.1603 * Blue - 0.2819 * Green - 0.4934 * Red + 0.7940 * NIR - 0.0002 * SWIR1 - 0.1446 * SWIR2$ $TCB = 0.2043 * Blue + 0.4158 * Green + 0.5524 * Red + 0.5741 * NIR + 0.3124 * SWIR1 + 0.2303 * SWIR2$	(Crist 1985; Powell et al. 2010)

vegetation index. The change in the index value due to the disturbance (Equation 1), hereafter referred to as the delta (d) was calculated as the difference between the value of the vegetation index in the growing season immediately following the disturbance (VI_t) and the reference index value (VI_{pre}). The recovery of the index value one year after disturbance (Equation 2), referred to as the recovery, was calculated by subtracting the value of the vegetation index taken from the disturbance composite (VI_t) to its value in the second growing season following the disturbance, taken from the post-disturbance composite (VI_{t+1}).

$$dVI = VI_{pre} - VI_t \quad (1)$$

$$VI \text{ recovery} = VI_{t+1} - VI_t \quad (2)$$

Recovery was included in the current study because the persistence of the changes in the canopy spectral reflectance has proven useful in discriminating between disturbance agents (Coops et al. 2020).

Modeling

Attribution of the disturbance agent

Multinomial logistic regression (MLR) was used to investigate how the Landsat-derived metrics could allow discriminating between the effects of the two disturbances and differentiate stands that were disturbed from those that remained undisturbed. MLR is an extension of binary logistic regression used when the categorical dependent variable has more than two categories. The outcome from MLR is a probability associated with each class of the dependent variable (Jobson 2012). MLR has been used extensively to solve classification problems in environmental and remote sensing studies, for instance, to classify land cover types from satellite imagery (e.g., McRoberts 2011) soil types from topographic data (DeBella-Gilo and Etzelmüller 2009) and crop disease status using a hyperspectral radiometer (Prabhakar et al. 2013). The assumptions of MLR do not include normality,

linearity, or homoscedasticity, making it less restrictive than other classification methods used in remote sensing such as discriminant analysis. The results from MLR are also easy to interpret compared to the results of other machine learning approaches (Hogland et al. 2013). Penalized MLR was used in the current study because it allows removing the bias in the maximum likelihood estimates of the parameters when the number of outcome categories is large or, as in the current study, when the sample size is small (Bashir and Carter 2010; Firth 1993; Kosmidis and Firth 2011). In penalized MLR, a penalty function is applied to shrink the coefficients of the less contributive variables toward zero, reducing overfitting issues (de Jong et al. 2019).

A set of candidate models was built from the Landsat metrics calculated for the vegetation indices presented above. The reliability of penalized MLR remains affected by the number of events per variables (EPV), which represents the number of events in the smaller outcome group divided by the number of regression coefficients estimated. While no absolute recommendations have been formulated in the case of MLR, a conservative minimal number of EPV (i.e., 23) was maintained in the current study by including a maximum of two explanatory variables in the candidate models (Austin and Steyerberg 2017; de Jong et al. 2019). Only combinations of variables with a Pearson R coefficient under 0.7 were included in a given model. In the first group of candidate models, two delta metrics susceptible to be indicative of different changes in canopy condition were included, while a second group included both one delta and one recovery metric. Implementation of the models was done in the R programming environment using the 140 plots distributed in the three disturbance categories. The final model was identified after a model-selection procedure based on the Second-order Akaike Information Criterion (AICc) conducted using R package AICcmodavg (Mazerolle 2020).

Assessment of the severity of the disturbance

Examination of the data revealed a linear association between the dependent and independent variables. The assumptions of normality of the residuals and homoscedasticity were also fulfilled, it was deemed that ordinary least square regression was the most suitable and direct approach to create the disturbance-specific severity assessment models. Linear regression allowed modeling the severity of the disturbances as a continuous variable and the creation of easy-to-interpret models. A first group of candidate models was created for each disturbance type and included the delta metrics derived from either one or two vegetation indices, ensuring the Pearson R value remained under 0.7 when multiple predictors were included. To investigate the effect of the pre-disturbance stand condition on the relationship between disturbance severity and changes in the canopy spectral reflectance, we created a second group of candidate models that included the basal area of the plot prior to the disturbance as a covariate. Model selection based on AICc was conducted separately for both disturbance types but involved the same set of candidate models. The number of available permanent sample plots was deemed insufficient to split the data into training and validation datasets. Therefore, all 47 plots that sustained damage from the 1998 ice storm were used in the development of the model dedicated to the assessment of the damage to the canopy caused by the ice storm, hereafter referred to as the ice storm model. Likewise, all 46 plots that were harvested were used in the development of the model dedicated to the assessment of the basal area removal after partial harvesting, hereafter referred to as the partial harvest model. The normality of the residuals was verified graphically and using the Shapiro-Wilk test, while the assumption of homoscedasticity was verified using the Breusch-Pagan Test.

Model application

To visualize the behavior of the disturbance-specific models and how they can serve to illustrate the variability in disturbance severity at both the landscape and stand levels, we mapped the predicted damage from disturbance events at specific locations within the study area. The selected subsets of our study area are located southwest of Lake Megantic in Southern Quebec (Figure 2(a)). This area was affected by the severe ice storm of 1998, and damage to the canopy ranging from light to severe was confirmed over the region by an aerial survey conducted in February

1998 (Chabot et al. 1998; Majcen et al. 1999). In the same region, we also selected six adjacent stands totaling 373.4 ha, in which partial harvest operations were conducted in 2020, after the end of the growing season (Figure 2(b)).

Landsat composites representing the reference and disturbance periods were created using the GEE implementation of the best available pixel (BAP) composite algorithm (White et al. 2014), allowing the creation of cloud-free, radiometrically and phenologically consistent surface reflectance composites, which are spatially contiguous over the targeted areas. As in the model-development step, two composites were first created for the two growing seasons preceding the disturbances. These composites were averaged to create a single composite representing the reference condition of the forest. The reference composite used to assess the severity of the damage caused by the ice storm of 1998, therefore, included pixels from the Landsat scenes acquired in the growing seasons of 1996 and 1997. The reference composite for the assessment of the basal area removal consecutively to the partial harvests included pixels from scenes acquired in the growing seasons of 2019 and 2020. Disturbance composites were created from scenes acquired in the growing season of 1998 for the ice storm-affected area, and 2021 for the harvested area. The vegetation indices and their associated delta metrics included as predictors in the ice storm and partial harvest models were then calculated from the reference and disturbance composites.

The ice storm model was applied to all broadleaved dominated stands of the area that had not been harvested in that same year. The sum of stands meeting these criteria had a combined area of 3974.1 ha in the first application subset. Using data from the forest inventory layer and a one-meter digital elevation model, we analyzed how the damage to the canopy predicted using the ice storm model varied as a function of biophysical characteristics such as the stand age, species composition, elevation and slope aspect. Analyses of variance and multiple comparisons with the Tukey honestly significant difference (HSD) test were used to investigate for statistically significant differences. The partial harvest model was applied to the six stands harvested in 2020, where the basal area removal levels ranged from 24% to 39% depending on the stand. Predictions from the model were averaged at the stand level, using polygons from the forest inventory layer, and compared to the post-harvest inventory data included in the geospatial layer made available by the landowner.

Results

Attribution of the disturbance causal agent

Among the tested MLR candidate models for the attribution of the disturbance causal agent, the most accurate comprised the dNBR and dTCA as predictors (Table 5). The model yielded an overall accuracy of 82.9% (Table 6). The lowest producer's accuracy was obtained for undisturbed plots while the highest was obtained with the ice storm damage. A proportion of 22.0% of the undisturbed plots was misclassified as disturbed, while only 13.3% of the ice storm-damaged plots were misclassified either as undisturbed (11.1%) or harvested (2.2%). The producer's accuracy for the harvested plots lay in between, with 15.6% of misclassified plots, either as undisturbed (6.7%) or damaged by the ice storm (8.9%). The user's accuracy values were very similar for all three categories. A proportion of 17.0% of plots classified as undisturbed were actually disturbed plots. A same proportion of 17.0% of the plots classified as damaged by an ice storm was in reality harvested (8.5%) or undisturbed (8.5%) plots and 17.4% of the plots classified as harvested were, in

Table 5. Ranking of the candidate models for the assessment of ice storm damage.

Model ID	Model parameters	AICc	Δ_i	Mk	W_{t_i}
2	dNBR + dTCA	144.78	0.00	1.00	1.00
4	dTCW + dTCA	183.49	38.72	0.00	0.00
7	dNBR + NDVI recovery	205.61	60.83	0.00	0.00
3	dGRVI + dTCA	214.85	70.07	0.00	0.00
1	dNBR + dGRVI	222.84	78.07	0.00	0.00
6	dNBR + GRVI recovery	223.87	79.09	0.00	0.00
9	dTCW + NDVI recovery	227.95	83.17	0.00	0.00
5	dTCW + dGRVI	253.33	108.55	0.00	0.00
8	dGRVI + NDVI recovery	257.31	112.54	0.00	0.00
10	Intercept only	311.68	166.91	0.00	0.00

AICc is the Akaike Information Criteria, corrected for small sample sizes, with deltaAICc (Δ_i), model likelihood (Mk) and AICc weight (W_{t_i}). Values in bold indicate the model and associated explanatory variables that were retained after the model selection procedure

reality, undisturbed plots (15.2%) or plots that had sustained some level of damage from the ice storm (2.2%).

The confusion matrix is presented in Table 7, and the individual effect of the predictors included in the final model is shown in Figure 3. Pixels exhibiting a high dNBR value, but only minor to no change in TCA were identified as damaged from an ice storm, while pixels exhibiting a moderate change in NBR but a large variation in TCA were identified as harvested. Pixels for which both dNBR and dTCA values were small were identified as undisturbed.

Disturbance-specific models

Ice storm

The best-fit model among the tested candidates for assessing the severity of the damage to the canopy after the ice storm included two delta metrics, i.e., the difference in Tasseled Cap Wetness (dTCAW) and the difference in the Green-Red Vegetation Index (dGRVI). The selected model also included the

Table 6. Accuracy metrics and Kappa statistics for the selected multinomial classification model.

	Producer's accuracy (%)	User's accuracy (%)	Overall accuracy (%)	Kappa
Ice storm	86.7	83.0		
Harvested	84.4	82.6	82.9	0.74
Undisturbed	78.0	83.0		

Table 7. Confusion matrix after applying the multinomial classification model.

Reference/prediction	Control	Harvest	Ice storm
Control	39	3	5
Harvest	7	38	1
Ice storm	4	4	39

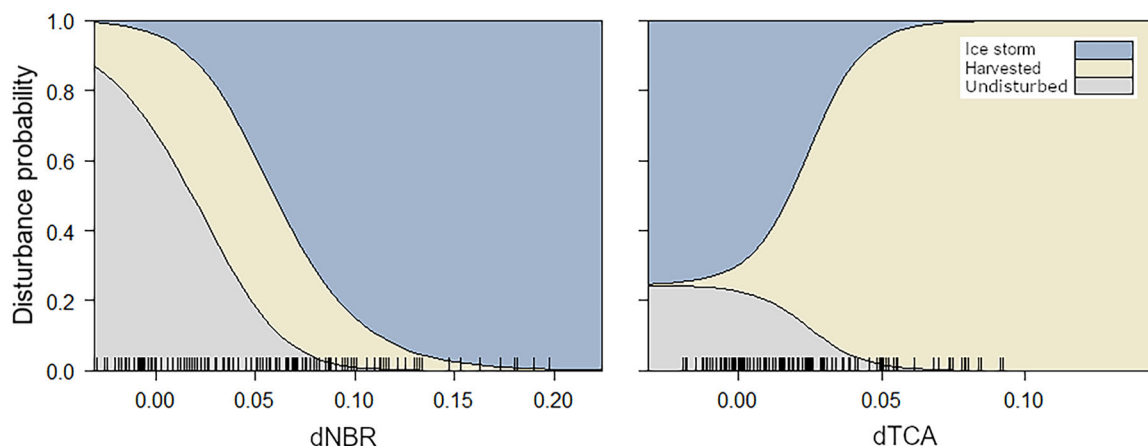


Figure 3. The individual effect of the predictors are included in the final disturbance classification model.

basal area of the plot prior to the disturbance as a covariate (Table 8).

The model reached an r -squared value of 0.59, with a root mean square error of 10.28. Estimates of the model parameters are shown in Table 9, while model predictions and unconditional 95% confidence intervals for the best-fit model parameters are shown in Figure 4. There was a positive relationship between the Landsat-derived metrics and the predicted damage to the canopy, and a higher basal area prior to the disturbance tended to be associated with lower damage for a given change in TCW and GRVI. High dTCW values combined with high dGRVI values and a low pre-disturbance basal area yielded the highest predicted damage to the canopy. The actual versus predicted damage to the canopy for the 47 plots used in model development is presented in Figure 5a.

Table 8. Ranking of the candidate models for the assessment of ice storm damage.

Model ID	Model parameters	AICc	Δi	Mk	Wt_i
12	dTCW + dGRVI + Pre-disturbance BA	363.95	0.00	1.00	0.68
9	dNBR + dGRVI + Pre-disturbance BA	366.59	2.65	0.27	0.18
7	dTCW + dGRVI	367.47	3.52	0.17	0.12
5	dNBR + dGRVI	371.12	7.17	0.03	0.02
10	dNBR + Pre-disturbance BA	379.83	15.88	0.00	0.00
3	dGRVI	380.28	16.33	0.00	0.00
1	dNBR	381.43	17.48	0.00	0.00
8	dTCW + dGRVI	381.90	17.95	0.00	0.00
6	dNDVI + dNBR	383.00	19.05	0.00	0.00
2	dNDVI	383.87	19.92	0.00	0.00
4	dTCW	386.14	22.20	0.00	0.00
11	dTCW + Pre-disturbance BA	386.36	22.42	0.00	0.00
13	Intercept only	401.51	37.56	0.00	0.00

AICc is the Akaike Information Criteria, corrected for small sample sizes, with deltaAICc (Δi), model likelihood (Mk) and AICc weight (Wt_i).

Values in bold indicate the model and associated explanatory variables that were retained after the model selection procedure.

Table 9. Estimates and standard error (SE) for the best-fit ice storm model parameters.

Parameter	Estimate	SE
dTCW	0.048	0.012
dGRVI	280.71	51.18
Intercept	22.16	7.45

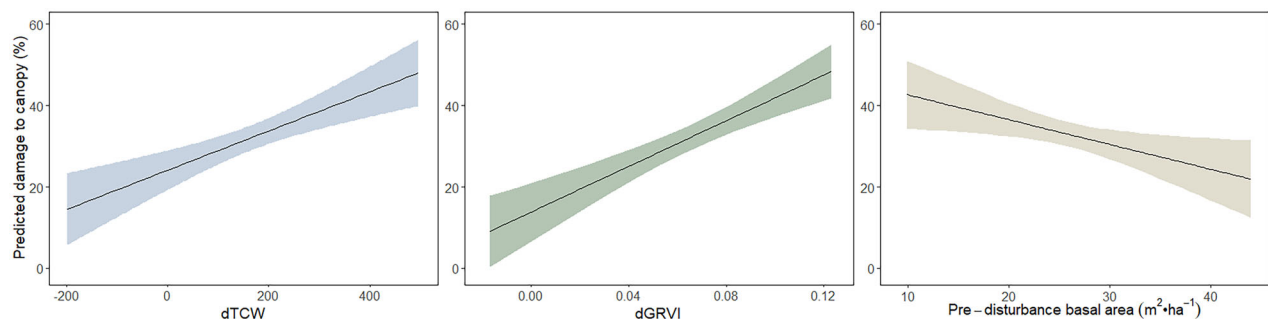


Figure 4. Model predictions and unconditional 95% confidence intervals for the best-fit model parameters for ice storm damage.

Model application – area damaged by the ice storm of 1998

Although the basal area of the stand prior to the disturbance was among the predictors retained in the ice storm model, this information was not available in the historical forest inventory layers available for the study site. We, therefore, applied the predictions of the third-ranked model, which included only the two delta metrics from the best-fit model, and had a relatively small difference in AICc ($\Delta i = 3.52$) compared to the first-ranked model (Figure 6). The median of the predicted damage to the canopy over the area of application of our model was 26.3% and 79.9% of pixels (3175.7 ha) were deemed to have sustained over 10% of damage to the canopy. The predicted damage was lower than 50% in 90% of the area.

Within the model application area, young even-aged stands exhibited a significantly lower ($p < 0.0001$) average level of damage to the canopy than other stand types. Stands that were harvested either by clearcutting or strip cutting in the fifteen years prior to the ice storm had a predicted average damage to the canopy of 15.3% compared to 25.1% for other stand types. Similarly, the analysis of variance conducted over the area revealed that broadleaved-dominated mixed stands sustained significantly ($p < 0.001$) less damage than pure broadleaved stands during this disturbance event, with predicted proportions of damage to the canopy of 23.4 and 26.5%, respectively. There was also a significant difference ($p < 0.0001$) between the levels of damage predicted in stands at lower altitudes (≤ 500 m, 23.1%) and stands located at higher altitudes where predictions were higher (> 500 m, 29.4%). The slope aspect also had a significant ($p < 0.001$) effect on the level of damage as stands sustained higher damage on slopes facing East or South (29.1% and 28.4%, respectively) compared to stands either on North (24.1%) or West (24.1%) facing slopes.

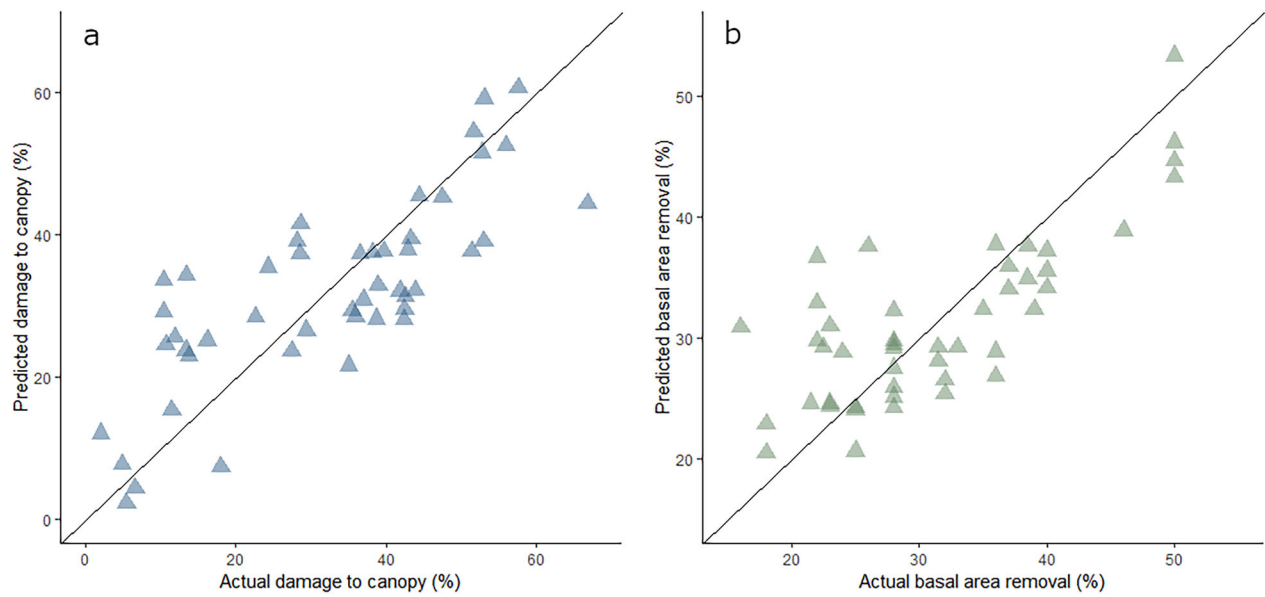


Figure 5. (a) Actual versus predicted damage to the canopy of the 47 plots included in the development of the ice storm model (b) Actual versus predicted basal area removal of the 46 plots included in the development of the partial harvest model. The solid line represents the 1:1 relationship.

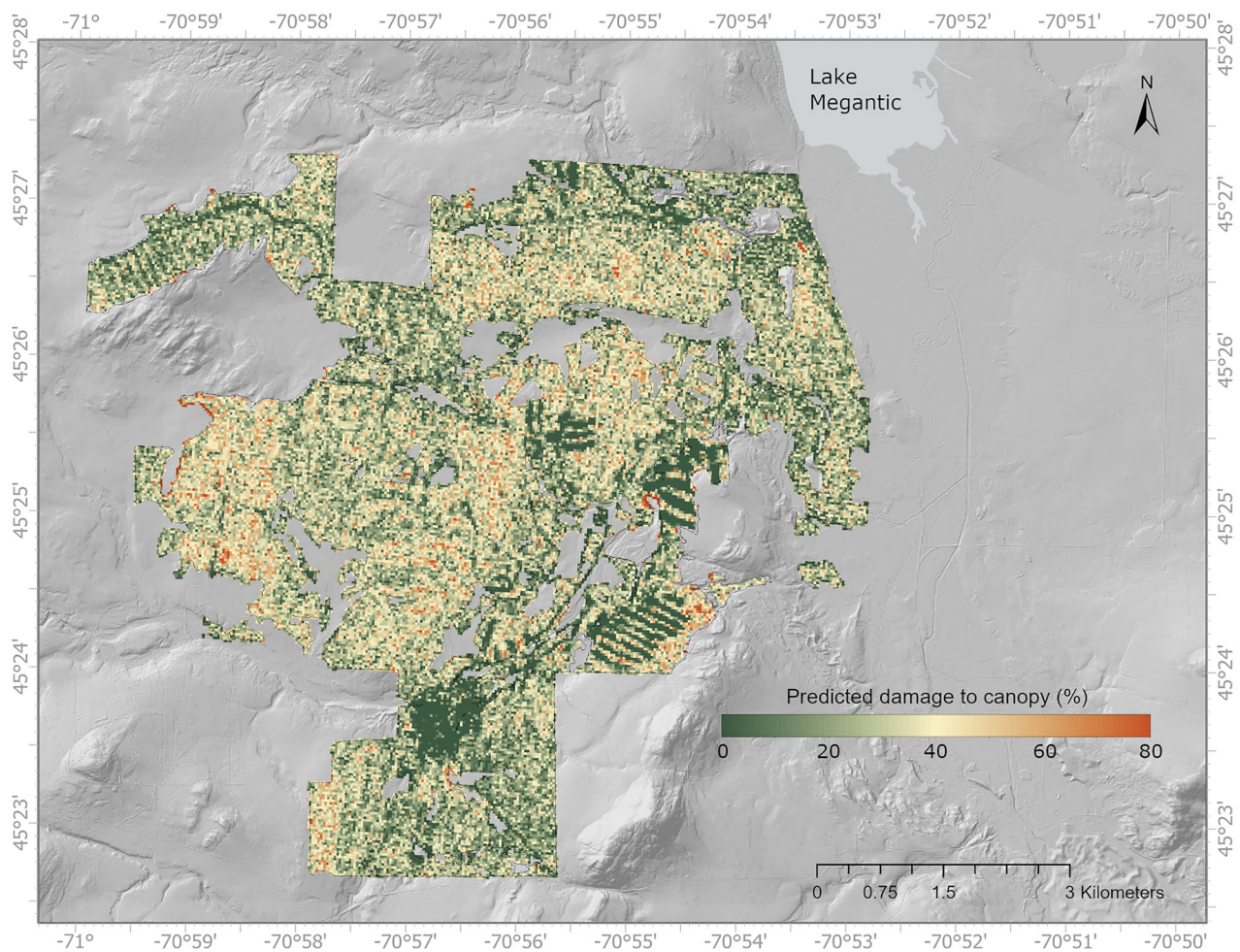


Figure 6. Predicted damage to canopy (%) consequently to the ice storm of 1998 over a subset of the study area.

Table 10. Ranking of the candidate models for the assessment of basal area removal.

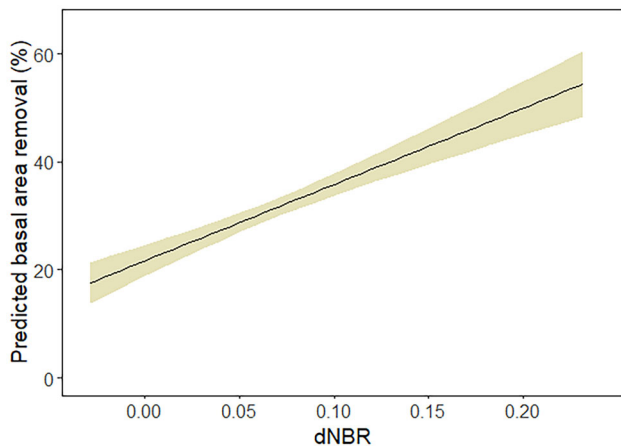
Model ID	Model parameters	AICc	Δ_i	Mk	W_{t_i}
1	dNBR	298.23	0.00	1.00	0.25
10	dNBR + Pre-disturbance BA	299.04	0.81	0.67	0.17
5	dNBR + dGRVI	299.50	1.26	0.53	0.13
12	dTCW + dGRVI + Pre-disturbance BA	299.51	1.28	0.53	0.13
8	dTCW + dGRVI	300.20	1.97	0.37	0.09
6	dNDVI + dNBR	300.28	2.05	0.36	0.09
9	dNBR + dGRVI + Pre-disturbance BA	300.41	2.17	0.34	0.08
11	dTCW + Pre-disturbance BA	302.41	4.18	0.12	0.03
4	dTCW	303.11	4.88	0.09	0.02
7	dTCW + dNDVI	304.98	6.75	0.03	0.01
2	dNDVI	324.34	26.11	0.00	0.00
3	dGRVI	326.65	28.42	0.00	0.00
13	Intercept only	336.25	38.02	0.00	0.00

AICc is the Akaike Information Criteria, corrected for small sample sizes, with deltaAICc (Δ_i), model likelihood (Mk) and AICc weight (W_{t_i}).

Values in bold indicate the model and associated explanatory variables that were retained after the model selection procedure.

Table 11. Estimates and standard error (SE) for the best-fit partial harvest model parameters.

Parameter	Estimate	SE
dNBR	141.65	18.03
Intercept	21.66	1.50

**Figure 7.** Model predictions and unconditional 95% confidence intervals for the best-fit model parameter for partial harvest.

Partial harvest

Among the tested candidates, the best-fit model for assessing the basal area removal from partial harvest included a single predictor i.e., the change in NBR value (dNBR, Table 10). The r-squared value of the final partial harvest model was 0.57, with a root mean square error of 5.76. Estimates of the model parameters are shown in Table 11, and model predictions and unconditional 95% confidence intervals for the model parameters are presented in Figure 7.

There was a positive relationship between dNBR and the harvested proportion of the basal area; the

removal of a greater proportion of the basal area resulted in larger dNBR values. The actual versus predicted basal area removal for the 46 plots used in model development is presented in Figure 5(b).

Model application – Area harvested in 2020

The selected partial harvest model was applied over the harvest area composed of six different stands that were harvested after the 2020 growing season (Figure 8).

The actual levels of basal area removal ranged from 24.0% to 39.0%, while the predicted removal levels ranged from 24.0% to 36.3% (Table 12). The absolute prediction error ranged from 0.7% to 16.6% for five stands out of six, but reached 38.5% in the case of stand E, for a median error of 12.6%.

Discussion

Attribution of the disturbance causal agent

The two disturbances included in this study led to contrasting changes in the canopy spectral reflectance. Our results show that a combination of Landsat-derived vegetation indices can help identify the causal agent of a disturbance. The final MLR classification model included two indices that are each associated with different changes within the canopy. The dNBR is increasingly used in disturbance detection algorithms, such as LandTrendr (Kennedy et al. 2010) and C2C (Hermosilla et al. 2015b) to detect both stand-replacing and non-stand-replacing disturbances. For the disturbance events investigated in the current study, the average dNBR value was greater for plots damaged by the ice storm than for harvested plots. This observation highlights the importance of correctly identifying the nature of a disturbance before assessing its severity. While the damage caused to crowns by an ice storm can be considerable, its impact on key ecological attributes, such as the amount of living biomass, is not comparable to that of a partial harvest where trees are removed from the stand. The larger variation in NBR observed in plots affected by the ice storm may be explained by the fundamentally different nature of the two types of disturbance. In the case of partial harvest, operations are usually conducted through a limited number of logging trails in which the machinery operates. The basal area removal is mainly concentrated within these trails (Moreau et al. 2019), which can be occluded from airborne observations by the crowns of the residual trees. As the targeted basal area removal increases, more trees are going to be harvested

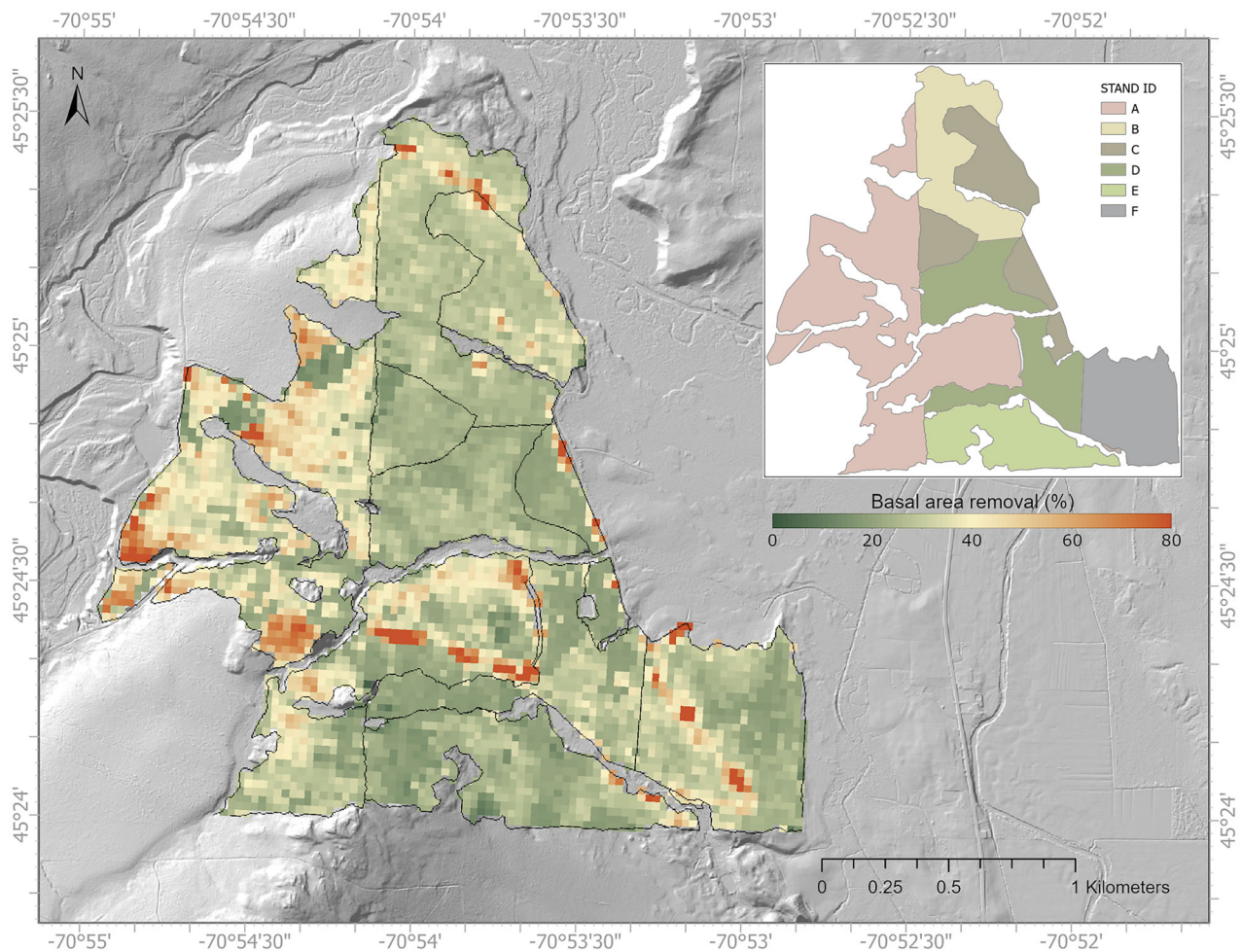


Figure 8. Predicted basal area removal (%) over the area harvested in 2020 within the study site.

Table 12. Actual and predicted basal area removal for the stands within the cut block (area) harvested in 2020.

Stand ID	Area (ha)	Initial BA ($\text{m}^2 \cdot \text{ha}$)	Final BA ($\text{m}^2 \cdot \text{ha}$)	Actual BA removal (%)	Predicted BA removal (%)	Absolute error (%)
A	140.5	19.3	12.0	37.8	36.3	4.2
B	43.6	26.4	17.1	35.2	29.4	16.6
C	48.8	19.1	13.8	27.7	27.6	0.7
D	57.4	26.6	20.6	22.6	25.4	12.6
E	38.7	20.5	12.5	39.0	24.0	38.5
F	43.8	26.4	17.1	35.2	29.8	15.3

between the trails. The effect on the canopy spectral reflectance varies locally and may be relatively subtle at a 30 m resolution (Franklin et al. 2001). While the damage caused to the canopy after an ice storm is also variable, the freezing rain is distributed uniformly, at least at the plot scale, and hits the upper layer of the canopy first. Broken branches and the associated decrease in leaf area index (LAI) may therefore be captured more easily through airborne observations than the effect of partial harvesting. Despite this contrast between disturbance types, the range of dNBR values of plots that were affected by the ice storm ($-0.01 \leq \text{dNBR} \leq 0.20$) remained very similar to

that of plots that were harvested ($-0.01 \leq \text{dNBR} \leq 0.22$). The inclusion of the dTCA in the model allowed a better differentiation of the respective effects of both disturbances. Indeed, the overlap in dTCA values between plots damaged by the ice storm ($-0.04 \leq \text{dTCA} \leq 0.02$) and harvested plots ($-0.01 \leq \text{dTCA} \leq 0.14$) was very small. The dTCA was significantly higher ($p < 0.0001$) in harvested stands compared to stands affected by the ice storm, while there were no significant differences ($p = 0.70$) in dTCA between the latter and the undamaged plots. These results are in line with previous studies that used the TCA as an estimator of living biomass and forest

cover density (Ahmed et al. 2014; Gómez et al. 2011; Powell et al. 2010). Although an ice storm causes damage to tree crowns, it does not affect the structure of a stand in the way a partial harvest does.

Disturbance-specific models

The Landsat-derived indices included in the final disturbance-specific models allowed assessing the severity of both types of disturbances in a continuous manner with a moderate proportion of the variance is accounted for. The partial harvest model relied on the dNBR as a single predictor. This index has been previously used to study partial harvesting in different ecosystems (Jarron et al. 2017; Tortini et al. 2019) and to monitor recovery following stand-replacing disturbances in boreal forests (Pickell et al. 2016; White et al. 2018). Our results suggest this index is appropriate to measure the intensity of partial harvests in northern hardwood forests. The NBR is a normalized difference of the Landsat near-infrared and second shortwave-infrared bands. Photosynthetically active vegetation shows a high reflectance in the near-infrared region compared to soil or non-photosynthetic vegetation (Clevers 1988). Soil and non-photosynthetic vegetation such as stems and branches show higher reflectance in the shortwave infrared regions compared to photosynthetically active vegetation, due to fewer water absorption features (Asner 1998). Partial harvest reduces the number of living trees and exposes bare soil and dry wooden debris, increasing the spectral reflectance in both the near-infrared and shortwave infrared regions of the spectrum, resulting in lower NBR as harvest proportion increases. It was challenging to assess the intensity of harvests with less than 30% of the basal area removed. At such low levels of harvest, the intensity was generally overestimated. This may be attributable to the presence of harvest trails in which all trees are removed to allow the machinery to circulate. In low-intensity partial harvests, the removal of trees within trails can be sufficient to reach the targeted basal area removal (Moreau et al. 2019). The canopy opening in logging trails may cause a substantial reduction in NBR values compared to the pre-harvest conditions, even at low levels of harvest. The additional removal of trees between the trails in harvests of higher intensity may produce more subtle variations in the index value.

The first-ranked model for the assessment of canopy damage due to the ice storm included two Landsat-derived indices i.e., the dTCW and dGRVI, in

addition to the pre-disturbance basal area of the stand. The TCW was found to be a good indicator of the structural attributes and development stage in closed canopy forests (Cohen et al. 1995; Czerwinski et al. 2014; Jin and Sader 2005), and is also used in disturbance detection algorithms (e.g., LandTrendr, Kennedy et al. 2010). When exploring the relationships between the TCW and the structure of various forest stands, Hansen et al. (2001) found that it was strongly correlated to attributes such as crown closure, average crown diameter and structural complexity, all of which are likely to be altered in a stand damaged by an ice storm.

The GRVI has been used as an indicator of seasonal changes in foliage in broadleaved forests and is considered an indicator of the photosynthetic rate of the canopy (Motohka et al. 2010; Muraoka et al. 2013; Yin et al. 2022). Its relevance for assessing damage to crowns is in line with the effects of an ice storm on the spectral reflectance of the canopy. Forest canopies impacted by ice storms experience a reduction in LAI that can last for up to two years after the event, because of the physical damage caused to stems and branches (Rhoads et al. 2002; Zarnovican 2002). Photosynthetically active vegetation strongly absorbs visible light and shows particularly strong absorption features in the red region (Clevers 1988; Federer and Tanner 1966). Damage to the canopy results in a decrease in these strong absorption features, captured in the red spectral reflectance band, and as a consequent lowering of GRVI values. The relationship between changes in LAI and spectral reflectance of forest canopies in the red region has been observed in several studies involving both satellite and aerial imagery, some of which were conducted consecutively to ice storms (King et al. 2005; Nemani et al. 1993; Pellikka et al. 2000; Rautiainen 2005).

Influence of the pre-disturbance basal area

The basal area of the stands prior to the disturbance influenced the relationships between the severity of the disturbance and the Landsat-derived metrics only in the case of ice storm damage. For the same level of damage to the canopy measured on the ground, dTCW and dGRVI values were higher in stands with a higher pre-disturbance basal area. The steeper relationship between the delta indices and the damage to crowns could be attributable to a more complex vertical structure in stands of high basal area. During an ice storm, the larger trees, which form the top layer of the canopy, are generally the most damaged (King et al. 2005; Rhoads et al. 2002). Therefore, the nature

of satellite-based vegetation indices, which are mainly focused on the upper layer in closed-canopy forests, could cause an overestimation of the damage, while trees in the lower layers, less visible from airborne observation, are likely to have sustained less damage.

Model application

Using disturbance-specific models to map the intensity of ice storm damage and partial harvesting over a subset of the study area revealed within-stand variability in both the damage to the canopy and harvest intensity. Consecutively to an ice storm, different levels of damage to the canopy may require specific silvicultural actions to restore the health and vigor of the stands and to account for the changes in the light regime caused by the disturbance. In severely damaged stands, salvage harvesting operations may be required to prevent losses due to mortality or degradation (Boulet et al. 2000; Bragg et al. 2003). Information on damage to the canopy at this resolution would therefore be useful in planning such interventions without the need to deploy a costly, time-consuming field sampling assessment. The application of the ice storm model over a large area allowed concluding significant correlations between biophysical variables and the level of damage to the canopy. In the case study dedicated to the ice storm event, young even-aged stands were less affected than older stands, which is in line with previous findings concluding that even-aged stands in northern hardwood forests are at low risk of damage from ice storms until they reach an age of 15–20 years (Pellikka et al. 2000; Rhoads et al. 2002). A comparison of the level of damage sustained by pure broadleaved stands compared to stands composed of a proportion of conifers revealed significant differences between the two groups, which is also consistent with findings from previous studies on the subject (Millward and Kraft 2004; Van Dyke 1999). The higher level of damage to the canopy for stands located at a higher elevation and the differences in damage between stands located on slopes facing different directions also agrees with what was found by other authors (Isaacs et al. 2014; King et al. 2005; Rhoads et al. 2002).

Regarding the application of the partial harvest model, the predicted basal area removal level was in general consistent with data from field inventories conducted consecutively to the harvest operations, with a median absolute error of 12.6%. Overall, the proportion of the basal area harvested tended to be slightly underestimated, although this was mainly the

case for one stand in which the difference between the predicted and actual level of the harvest was quite large. An indication that the model allowed a representative visualization of the variability of basal area removal within and between stands comes from the fact that Figure 8 showed a clear distinction between the silvicultural treatments that were applied in the harvest area. The higher level of variability of harvest levels in stand A, for example, was the result of a form of salvage logging, which aimed to recover unhealthy stems in a depleted stand. This resulted in higher spatial variability in basal area removal compared to other stands, which were all subjected to selection cuts characterized by a more uniform basal area removal to favor shade-tolerant species (Leak et al. 2014; Nyland 1998).

Limitations and needs for future research

The study of non-stand replacing disturbances through remote sensing remains at its early stages, especially in broadleaved forests where most of the previous work has focused on a single disturbance agent. The current study proposes a hurdle approach in which disturbances are first detected and attributed to a causal agent using MLR before disturbance-specific linear models are used to estimate the severity of the disturbance as a continuous variable. Although the decision to model severity as a continuous variable has the advantage of revealing fine spatial variability in the severity of the disturbances, the proposed disturbance-specific models only explained a moderate proportion of the variance. Addressing some of the limitations raised in this section could help increase our ability to estimate more accurately the level of change caused to forest ecosystems by non-stand replacing disturbances and to attribute their causal agents.

The range in severity of the disturbance events included in the current study was dictated by the occurrence of such events during the study period and the availability of data from the permanent sample plots. Conclusions on the accuracy of the approach used to attribute the causal agent to the disturbances are therefore only applicable considering the specific distribution of severity among the disturbances included in the sample. Likewise, the establishment of a threshold for detectability of damage to the canopy or basal area removal using the MLR model falls beyond the scope of the current study. Additional work is needed to identify such a threshold and how it may vary between different types of disturbances.

The relevance of a severity threshold should also be investigated in the case of disturbance-specific models, especially for partial harvests, for which the intensity was challenging to assess accurately when the BA removal was low.

While only two types of non-stand replacing disturbances were included in the current study, northern hardwood forests are subjected to other types of small- to moderate-scale disturbances from various causal agents such as insects and wind. The detectability of these disturbances and the possibility to distinguish their effect on the spectral reflectance of the canopy using the limited set of vegetation indices tested in this study needs to be investigated. The success of such an undertaking is likely influenced by the time of the year when the disturbance occurs. In the context of the present study, this is especially relevant for the partial harvest. Operations conducted during the winter on a snow cover may preserve the understory vegetation, which will benefit from the opening of the canopy and proliferate during the following growing season. Changes to the spectral reflectance of the canopy consecutively to such harvests may be more subtle than for harvests conducted within the growing season, for which the bare soil is more likely to be exposed by the circulation of the machinery (Wolf et al. 2008).

Our results have also shown that, in the case of an ice storm, the condition of the stands prior to the disturbance must be considered in the estimation of the damage caused to the canopy. There is a need to further investigate how this affects the accuracy of methods used to study non-stand replacing disturbances using satellite imagery and to better understand how it may vary among causal agents and forest types. To that extent, the retrospective estimation of forest structural attributes including basal area using Landsat time series in combination with other remote sensing tools (e.g., Matasci et al. 2018), appears promising, since it could provide valuable information on initial stand conditions when there is a lack of historical field inventory data.

Conclusions

Results from the current study confirm the feasibility and relevance of using Landsat-derived vegetation indices to discriminate between two different types of non-stand replacing disturbances in northern hardwood forests and assess their severity. Using a combination of vegetation indices allowed capturing differences in the effects of two non-stand replacing

disturbances on the spectral reflectance of the canopy. Our results confirmed the importance of identifying the causal agent before assessing the severity of a disturbance. For instance, the range of dNBR, one of the most commonly used metrics in disturbance detection, was very similar for plots that sustained damage after an ice storm and plots that were harvested. Yet, the effects of these two disturbances on the ecosystem dynamics are contrasting, both in their persistence and in severity. The different effects of ice storms and partial harvests on the spectral reflectance of the canopy have translated into the inclusion of a distinct set of predictors in the disturbance-specific severity assessment models. The application of these models over a subset of the study allowed for generating information on the spatial variability of the disturbances at a finer resolution than what is generally available to forest practitioners. This information could be useful in the planning and application of adapted silvicultural practices.

Acknowledgments

We would like to thank the staff from Domtar Corporation for their support on the project and for sharing inventory and harvest operations data.

Disclosure statement


No potential conflict of interest was reported by the author(s).

Funding

This work was supported by the NSERC Alliance project Silva21 NSERC ALLRP 556265–20, grantee Prof. Alexis Achim and by the NSERC Alexander Graham Bell Graduate Scholarships-Doctoral Program (CGS-D), award holder Alexandre Morin-Bernard.

ORCID

Alexis Achim  <http://orcid.org/0000-0003-0118-1651>

Nicholas C. Coops  <http://orcid.org/0000-0002-0151-9037>

References

- Ahmed, O.S., Franklin, S.E., and Wulder, M.A. 2014. "Integration of lidar and landsat data to estimate forest canopy cover in coastal British Columbia." *Photogrammetric Engineering & Remote Sensing*, Vol. 80(No. 10): pp. 953–961. doi:10.14358/PERS.80.10.953.
- Ahmed, O.S., Wulder, M.A., White, J.C., Hermosilla, T., Coops, N.C., and Franklin, S.E. 2017. "Classification of annual non-stand replacing boreal forest change in Canada using Landsat time series: A case study in

- northern Ontario.” *Remote Sensing Letters*, Vol. 8(No. 1): pp. 29–37. doi:10.1080/2150704X.2016.1233371.
- Asner, G.P. 1998. “Biophysical and biochemical sources of variability in canopy reflectance.” *Remote Sensing of Environment*, Vol. 64(No. 3): pp. 234–253. doi:10.1016/S0034-4257(98)00014-5.
- Austin, P.C., and Steyerberg, E.W. 2017. “Events per variable (EPV) and the relative performance of different strategies for estimating the out-of-sample validity of logistic regression models.” *Statistical Methods in Medical Research*, Vol. 26(No. 2): pp. 796–808. doi:10.1177/0962280214558972.
- Banskota, A., Kayastha, N., Falkowski, M.J., Wulder, M.A., Froese, R.E., and White, J.C. 2014. “Forest monitoring using landsat time series data: A review.” *Canadian Journal of Remote Sensing*, Vol. 40(No. 5): pp. 362–384. doi:10.1080/07038992.2014.987376.
- Bashir, S., and Carter, E.M. 2010. “Penalized multinomial mixture logit model.” *Computational Statistics*, Vol. 25(No. 1): pp. 121–141. doi:10.1007/s00180-009-0165-9.
- Bennett, I. 1959. *Glaze: Its Meteorology and Climatology, Geographical Distribution, and Economic Effects* (Vol. 4). New York, NY, USA: Headquarters, Quartermaster Research & Engineering Command, US Army.
- Boulet, B., Trottier, F., and Roy, G. 2000. *L'aménagement des peuplements forestiers touchés par le verglas*. Ministère des Ressources naturelles, Québec, p. 66. Québec: Ministère des Ressources naturelles du Québec.
- Bowman, D.M.J.S., Brienen, R.J.W., Gloor, E., Phillips, O.L., and Prior, L.D. 2013. “Detecting trends in tree growth: Not so simple.” *Trends in Plant Science*, Vol. 18(No. 1): pp. 11–17. doi:10.1016/j.tplants.2012.08.005.
- Bragg, D.C., Shelton, M.G., and Zeide, B. 2003. “Impacts and management implications of ice storms on forests in the southern United States.” *Forest Ecology and Management*, Vol. 186(No. 1–3): pp. 99–123. doi:10.1016/S0378-1127(03)00230-5.
- Burnett, J. S. 2002. *Assessing ice storm damage to hardwood forest canopies using the Advanced Solid-State Array Spectroradiometer (ASAS) and Landsat TM imagery*. PhD Thesis. Durham, NH, USA: University of New Hampshire.
- Chabot, M., Thériault, G., and Deschamps, L. 1998. *Forest damage caused by the ice storm of January 1998 - preliminary results of aerial reconnaissance carried out between January 19 and February 4, 1998*, 15. Direction de la conservation des forêts, Ministère des Ressources Naturelles, de la Faune et des Parcs. Québec, QC, Canada: Gouvernement du Québec.
- Clevers, J.G.P.W. 1988. “The derivation of a simplified reflectance model for the estimation of leaf area index.” *Remote Sensing of Environment*, Vol. 25(No. 1): pp. 53–69. doi:10.1016/0034-4257(88)90041-7.
- Cohen, W.B., Spies, T.A., and Fiorella, M. 1995. “Estimating the age and structure of forests in a multi-ownership landscape of western Oregon, U.S.A.” *International Journal of Remote Sensing*, Vol. 16(No. 4): pp. 721–746. doi:10.1080/01431169508954436.
- Coops, N.C., Shang, C., Wulder, M.A., White, J.C., and Hermosilla, T. 2020. “Change in forest condition: Characterizing non-stand replacing disturbances using time series satellite imagery.” *Forest Ecology and Management*, Vol. 474: pp. 118370. doi:10.1016/j.foreco.2020.118370.
- Coppin, P.R., and Bauer, M.E. 1996. “Digital change detection in forest ecosystems with remote sensing imagery.” *Remote Sensing Reviews*, Vol. 13(No. 3–4): pp. 207–234. doi:10.1080/02757259609532305.
- Crist, E.P. 1985. “A TM Tasseled Cap equivalent transformation for reflectance factor data.” *Remote Sensing of Environment*, Vol. 17(No. 3): pp. 301–306. doi:10.1016/0034-4257(85)90102-6.
- Crist, E.P., and Cicone, R.C. 1984. “A physically-based transformation of thematic mapper data—the TM Tasseled Cap.” *IEEE Transactions on Geoscience and Remote Sensing*, Vol. GE, Vol. 22(No. 3): pp. 256–263. doi:10.1109/TGRS.1984.350619.
- Czerwinski, C.J., King, D.J., and Mitchell, S.W. 2014. “Mapping forest growth and decline in a temperate mixed forest using temporal trend analysis of Landsat imagery, 1987–2010.” *Remote Sensing of Environment*, Vol. 141: pp. 188–200. doi:10.1016/j.rse.2013.11.006.
- Dannehyrolles, V., Dupuis, S., Fortin, G., Leroyer, M., de Römer, A., Terrail, R., Vellend, M., et al. 2019. “Stronger influence of anthropogenic disturbance than climate change on century-scale compositional changes in northern forests.” *Nature Communications*, Vol. 10(No. 1): Article 1. doi:10.1038/s41467-019-09265-z.
- de Jong, V.M.T., Eijkemans, M.J.C., van Calster, B., Timmerman, D., Moons, K.G.M., Steyerberg, E.W., and van Smeden, M. 2019. “Sample size considerations and predictive performance of multinomial logistic prediction models.” *Statistics in Medicine*, Vol. 38(No. 9): pp. 1601–1619. doi:10.1002/sim.8063.
- Debella-Gilo, M., and Etzelmüller, B. 2009. “Spatial prediction of soil classes using digital terrain analysis and multinomial logistic regression modeling integrated in GIS: Examples from Vestfold County, Norway.” *CATENA*, Vol. 77(No. 1): pp. 8–18. doi:10.1016/j.catena.2008.12.001.
- Federer, C.A., and Tanner, C.B. 1966. “Spectral distribution of light in the forest.” *Ecology*, Vol. 47(No. 4): pp. 555–560. doi:10.2307/1933932.
- Firth, D. 1993. “Bias reduction of maximum likelihood estimates.” *Biometrika*, Vol. 80(No. 1): pp. 27–38. doi:10.1093/biomet/80.1.27.
- Franklin, S.E., Lavigne, M.B., Moskal, L.M., Wulder, M.A., and McCaffrey, T.M. 2001. “Interpretation of forest harvest conditions in New Brunswick using landsat TM enhanced wetness difference imagery (EWDI).” *Canadian Journal of Remote Sensing*, Vol. 27(No. 2): pp. 118–128. doi:10.1080/07038992.2001.10854926.
- Franklin, S.E., Moskal, L., Lavigne, M., and Pugh, K. 2000. “Interpretation and classification of partially harvested forest stands in the Fundy model forest using multitemporal Landsat TM digital data.” *Canadian Journal of Remote Sensing*, Vol. 26(No. 4): pp. 318–333.
- Gardiner, B., and Moore, J. 2014. “Creating the wood supply of the future”. In *Challenges and Opportunities for the World's Forests in the 21st Century*, edited by T. Fenning, pp. 677–704. Dordrecht, Netherlands: Springer Netherlands. doi:10.1007/978-94-007-7076-8_30.
- Gillis, M.D., Omule, A.Y., and Brierley, T. 2005. “Monitoring Canada's forests: The national forest

- inventory.” *The Forestry Chronicle*, Vol. 81(No. 2): pp. 214–221. doi:10.5558/tfc81214-2.
- Gómez, C., White, J.C., and Wulder, M.A. 2011. “Characterizing the state and processes of change in a dynamic forest environment using hierarchical spatio-temporal segmentation.” *Remote Sensing of Environment*, Vol. 115(No. 7): pp. 1665–1679. doi:10.1016/j.rse.2011.02.025.
- Gorelick, N., Hancher, M., Dixon, M., Ilyushchenko, S., Thau, D., and Moore, R. 2017. “Google Earth Engine: Planetary-scale geospatial analysis for everyone.” *Remote Sensing of Environment*, Vol. 202: pp. 18–27. doi:10.1016/j.rse.2017.06.031.
- Gosselin, J. 2005. *Guide de reconnaissance des types écologiques de la région écologique 3d - Coteaux des basses Appalaches*. Québec, QC, Canada: Ministère des Ressources naturelles et de la Faune, Direction des inventaires forestiers, Division de la classification écologique et productivité des stations.
- Gosselin, J. 2007. *Guide de reconnaissance des types écologiques de la région écologique 2c - Coteaux de l’Estrie*. Québec, QC, Canada: Ministère des Ressources naturelles et de la Faune, Direction des inventaires forestiers, Division de la classification écologique et productivité des stations.
- Grayson, S. F., Buckley, D. S., Henning, J. G., Schweitzer, C. J., Gottschalk, K. W., and Loftis, D. L. 2012. “Understory light regimes following silvicultural treatments in central hardwood forests in Kentucky, USA”. *Forest Ecology and Management*, Vol. 279: pp. 66–76. doi:10.1016/j.foreco.2012.05.017.
- Hansen, M.J., Franklin, S.E., Woudsma, C., and Peterson, M. 2001. “Forest structure classification in the North Columbia Mountains using the landsat TM Tasseled Cap wetness component.” *Canadian Journal of Remote Sensing*, Vol. 27(No. 1): pp. 20–32. doi:10.1080/07038992.2001.10854916.
- Harvey, B.J., Andrus, R.A., and Anderson, S.C. 2019. “Incorporating biophysical gradients and uncertainty into burn severity maps in a temperate fire-prone forested region.” *Ecosphere*, Vol. 10(No. 2): p. e02600. doi:10.1002/ecs2.2600.
- Healey, S.P., Yang, Z., Cohen, W.B., and Pierce, D.J. 2006. “Application of two regression-based methods to estimate the effects of partial harvest on forest structure using Landsat data.” *Remote Sensing of Environment*, Vol. 101(No. 1): pp. 115–126. doi:10.1016/j.rse.2005.12.006.
- Hermosilla, T., Wulder, M.A., White, J.C., and Coops, N.C. 2015a. “Regional detection, characterization, and attribution of annual forest change from 1984 to 2012 using Landsat-derived time-series metrics.” *Remote Sensing of Environment*, Vol. 170: pp. 121–132. doi:10.1016/j.rse.2015.09.004.
- Hermosilla, T., Wulder, M.A., White, J.C., Coops, N.C., and Hobart, G.W. 2015b. “An integrated Landsat time series protocol for change detection and generation of annual gap-free surface reflectance composites.” *Remote Sensing of Environment*, Vol. 158: pp. 220–234. doi:10.1016/j.rse.2014.11.005.
- Hogland, J., Billor, N., and Anderson, N. 2013. “Comparison of standard maximum likelihood classification and polytomous logistic regression used in remote sensing.” *European Journal of Remote Sensing*, Vol. 46(No. 1): pp. 623–640.
- Irland, L.C. 1998. “Ice storm 1998 and the forests of the Northeast: A preliminary assessment.” *Journal of Forestry*, Vol. 96(No. 9): pp. 32–40.
- Isaacs, R.E., Stueve, K.M., Lafon, C.W., and Taylor, A.H. 2014. “Ice storms generate spatially heterogeneous damage patterns at the watershed scale in forested landscapes.” *Ecosphere*, Vol. 5(No. 11): p. art141. doi:10.1890/ES14-00234.1.
- Jarron, L.R., Hermosilla, T., Coops, N.C., Wulder, M.A., White, J.C., Hobart, G.W., and Leckie, D.G. 2017. “Differentiation of Alternate Harvesting Practices Using Annual Time Series of Landsat Data.” *Forests*, Vol. 8(No. 1): p. Article 1. doi:10.3390/f8010015.
- Jenkins, M. W., and Chambers, J. L. 1989. “Understory light levels in mature hardwood stands after partial overstory removal”. *Forest Ecology and Management*, Vol. 26(No. 4): pp. 247–256. doi:10.1016/0378-1127(89)90085-6.
- Jin, S., and Sader, S.A. 2005. “Comparison of time series Tasseled Cap wetness and the normalized difference moisture index in detecting forest disturbances.” *Remote Sensing of Environment*, Vol. 94(No. 3): pp. 364–372. doi:10.1016/j.rse.2004.10.012.
- Jobson, J. D. 2012. *Applied multivariate data analysis: volume II: Categorical and Multivariate Methods*. New York: Springer Science & Business Media.
- Johnson, E.W., and Ross, J. 2008. “Quantifying error in aerial survey data.” *Australian Forestry*, Vol. 71(No. 3): pp. 216–222. doi:10.1080/00049158.2008.10675038.
- Kennedy, R.E., Yang, Z., and Cohen, W.B. 2010. “Detecting trends in forest disturbance and recovery using yearly Landsat time series: 1. LandTrendr—temporal segmentation algorithms.” *Remote Sensing of Environment*, Vol. 114(No. 12): pp. 2897–2910. doi:10.1016/j.rse.2010.07.008.
- Key, C. H., and Benson, N. C., 2006. “Landscape assessment (LA)”. In *FIREMON: Fire Effects Monitoring and Inventory System. Gen. Tech. Rep. RMRS-GTR-164-CD*, edited by Lutes, D. C., Keane, R. E., Caratti, J. F., Key, C. H., Benson, N. C., Sutherland, S., and Gangi, L. J., p. LA-1–55, Vol. 164. Fort Collins, CO: US Department of Agriculture, Forest Service, Rocky Mountain Research Station.
- King, D.J., Olthof, I., Pellikka, P.K.E., Seed, E.D., and Butson, C. 2005. “Modelling and mapping damage to forests from an ice storm using remote sensing and environmental data.” *Natural Hazards*, Vol. 35(No. 3): pp. 321–342. doi:10.1007/s11069-004-1795-4.
- Kosmidis, I., and Firth, D. 2011. “Multinomial logit bias reduction via the Poisson log-linear model.” *Biometrika*, Vol. 98(No. 3): pp. 755–759. doi:10.1093/biomet/asr026.
- Leak, W. B., Yamasaki, M., and Holleran, R. 2014. “*Silvicultural guide for northern hardwoods in the northeast*”. *Gen. Tech. Rep. NRS-132*, 46 p., Vol. 132, pp. 1–46. Newtown Square, PA: US Department of Agriculture, Forest Service, Northern Research Station.
- Majcen, Z., Bédard, S., and Blais, L. 1999. *Domages causés par le verglas dans trois secteurs forestiers - Note de recherche no.95*. Québec, QC, Canada: Gouvernement du Québec, Ministère des ressources naturelles, Direction de la recherche forestière.

- Matasci, G., Hermosilla, T., Wulder, M.A., White, J.C., Coops, N.C., Hobart, G.W., Bolton, D.K., Tompalski, P., and Bater, C.W. 2018. "Three decades of forest structural dynamics over Canada's forested ecosystems using Landsat time-series and lidar plots." *Remote Sensing of Environment*, Vol. 216: pp. 697–714.
- Mazerolle, M. J. 2020. *AICcmodavg: Model selection and multimodel inference based on (Q)AIC(c)*. R package version 2.3-1. <https://cran.r-project.org/package=AICcmodavg>.
- McRoberts, R.E. 2011. "Satellite image-based maps: Scientific inference or pretty pictures?" *Remote Sensing of Environment*, Vol. 115(No. 2): pp. 715–724. doi:10.1016/j.rse.2010.10.013.
- Merrill, F.B. 1935. "BASAL AREA TREE AND LOG VOLUMES." *The Forestry Chronicle*, Vol. 21(No. 4): pp. 254–266.
- Millward, A.A., and Kraft, C.E. 2004. "Physical influences of landscape on a large-extent ecological disturbance: The northeastern North American ice storm of 1998." *Landscape Ecology*, Vol. 19(No. 1): pp. 99–111. doi:10.1023/B:LAND.0000018369.41798.2f.
- Moreau, G., Achim, A., and Pothier, D. 2019. "A dendro-chronological reconstruction of sugar maple growth and mortality dynamics in partially cut northern hardwood forests." *Forest Ecology and Management*, Vol. 437: pp. 17–26. doi:10.1016/j.foreco.2019.01.031.
- Motohka, T., Nasahara, K.N., Oguma, H., and Tsuchida, S. 2010. "Applicability of green-red vegetation index for remote sensing of vegetation phenology." *Remote Sensing*, Vol. 2(No. 10): p. Article 10. doi:10.3390/rs2102369.
- Muraoka, H., Noda, H.M., Nagai, S., Motohka, T., Saitoh, T.M., Nasahara, K.N., and Saigusa, N. 2013. "Spectral vegetation indices as the indicator of canopy photosynthetic productivity in a deciduous broadleaf forest." *Journal of Plant Ecology*, Vol. 6(No. 5): pp. 393–407. doi:10.1093/jpe/rts037.
- Nemani, R., Pierce, L., Running, S., and Band, L. 1993. "Forest ecosystem processes at the watershed scale: sensitivity to remotely-sensed Leaf Area Index estimates." *International Journal of Remote Sensing*, Vol. 14(No. 13): pp. 2519–2534. doi:10.1080/01431169308904290.
- Nyland, R.D. 1998. "Selection system in northern hardwoods." *Journal of Forestry*, Vol. 96(No. 7): pp. 18–21.
- Olthof, I., King, D.J., and Lautenschlager, R.A. 2004. "Mapping deciduous forest ice storm damage using Landsat and environmental data." *Remote Sensing of Environment*, Vol. 89(No. 4): pp. 484–496. doi:10.1016/j.rse.2003.11.010.
- Payette, S., Filion, L., and Delwaide, A. 1990. "Disturbance regime of a cold temperate forest as deduced from tree-ring patterns: The Tantaré Ecological Reserve, Quebec." *Canadian Journal of Forest Research*, Vol. 20(No. 8): pp. 1228–1241. doi:10.1139/x90-162.
- Pellikka, P., Seed, E.D., and King, D.J. 2000. "Modelling deciduous forest ice storm damage using aerial CIR imagery and hemispheric photography." *Canadian Journal of Remote Sensing*, Vol. 26(No. 5): pp. 394–405. doi:10.1080/07038992.2000.10855271.
- Peng, C., Ma, Z., Lei, X., Zhu, Q., Chen, H., Wang, W., Liu, S., Li, W., Fang, X., and Zhou, X. 2011. "A drought-induced pervasive increase in tree mortality across Canada's boreal forests." *Nature Climate Change* Vol. 1(No. 9): pp. 467–471. doi:10.1038/nclimate1293.
- Pickell, P.D., Hermosilla, T., Frazier, R.J., Coops, N.C., and Wulder, M.A. 2016. "Forest recovery trends derived from Landsat time series for North American boreal forests." *International Journal of Remote Sensing*, Vol. 37(No. 1): pp. 138–149. doi:10.1080/2150704X.2015.1126375.
- Powell, S.L., Cohen, W.B., Healey, S.P., Kennedy, R.E., Moisen, G.G., Pierce, K.B., and Ohmann, J.L. 2010. "Quantification of live aboveground forest biomass dynamics with Landsat time-series and field inventory data: A comparison of empirical modeling approaches." *Remote Sensing of Environment*, Vol. 114(No. 5): pp. 1053–1068. doi:10.1016/j.rse.2009.12.018.
- Prabhakar, M., Prasad, Y.G., Desai, S., Thirupathi, M., Gopika, K., Rao, G.R., and Venkateswarlu, B. 2013. "Hyperspectral remote sensing of yellow mosaic severity and associated pigment losses in *Vigna mungo* using multinomial logistic regression models." *Crop Protection*, Vol. 45: pp. 132–140. doi:10.1016/j.cropro.2012.12.003.
- Proulx, O. J., and Greene, D. F. 2001. The relationship between ice thickness and northern hardwood tree damage during ice storms. *Canadian Journal of Forest Research*, Vol. 31: 1758–1767.
- Rautiainen, M. 2005. "Retrieval of leaf area index for a coniferous forest by inverting a forest reflectance model." *Remote Sensing of Environment*, Vol. 99(No. 3): pp. 295–303. doi:10.1016/j.rse.2005.09.004.
- Rhoads, A.G., Hamburg, S.P., Fahey, T.J., Siccama, T.G., Hane, E.N., Battles, J., Cogbill, C., and Randall, J. 2002. "Effects of an intense ice storm on the structure of a northern hardwood forest." *Canadian Journal of Forest Research*, Vol. 32(No. 10): pp. 1763–1775. doi:10.1139/x02-089.
- Riahi, K., van Vuuren, D.P., Kriegler, E., Edmonds, J., O'Neill, B.C., Fujimori, S., Bauer, N., et al. 2017. "The Shared Socioeconomic Pathways and their energy, land use, and greenhouse gas emissions implications: An overview." *Global Environmental Change*, Vol. 42 pp. 153–168. doi:10.1016/j.gloenvcha.2016.05.009.
- Rodman, K.C., Andrus, R.A., Veblen, T.T., and Hart, S.J. 2021. "Disturbance detection in landsat time series is influenced by tree mortality agent and severity, not by prior disturbance." *Remote Sensing of Environment*, Vol. 254: pp. 112244. doi:10.1016/j.rse.2020.112244.
- Sader, S.A., Bertrand, M., and Wilson, E.H. 2003. "Satellite change detection of forest harvest patterns on an industrial forest landscape." *Forest Science*, Vol. 49(No. 3): pp. 341–353. doi:10.1093/forestscience/49.3.341.
- Saucier, J., Robitaille, A., and Grondin, P. 2009. "Cadre bioclimatique du Québec." *Manuel de Foresterie* Vol. 2: pp. 186–205.
- Seidl, R., Thom, D., Kautz, M., Martin-Benito, D., Peltoniemi, M., Vacchiano, G., Wild, J., et al. 2017. "Forest disturbances under climate change." *Nature Climate Change*, Vol. 7(No. 6): p. Article 6. doi:10.1038/nclimate3303.
- Seymour, R.S., White, A.S., and deMaynadier, P.G. 2002. "Natural disturbance regimes in northeastern North America—evaluating silvicultural systems using natural scales and frequencies." *Forest Ecology and Management*,

- Vol. 155(No. 1–3): pp. 357–367. doi:10.1016/S0378-1127(01)00572-2.
- Stueve, K.M., Lafon, C.W., and Isaacs, R.E. 2007. “Spatial patterns of ice storm disturbance on a forested landscape in the Appalachian Mountains, Virginia.” *Area*, Vol. 39(No. 1): pp. 20–30.
- Thom, D., and Seidl, R. 2016. “Natural disturbance impacts on ecosystem services and biodiversity in temperate and boreal forests.” *Biological Reviews of the Cambridge Philosophical Society*, Vol. 91(No. 3): pp. 760–781. doi:10.1111/brv.12193.
- Tortini, R., Mayer, A.L., Hermosilla, T., Coops, N.C., and Wulder, M.A. 2019. “Using annual Landsat imagery to identify harvesting over a range of intensities for non-industrial family forests.” *Landscape and Urban Planning*, Vol. 188: pp. 143–150. doi:10.1016/j.landurbplan.2018.04.012.
- Tucker, C.J. 1979. “Red and photographic infrared linear combinations for monitoring vegetation.” *Remote Sensing of Environment*, Vol. 8: p. 127.
- Turner, M.G. 2010. “Disturbance and landscape dynamics in a changing world.” *Ecology*, Vol. 91(No. 10): pp. 2833–2849. doi:10.1890/10-0097.1.
- Van Dyke, O. 1999. *A literature review of ice storm impacts on forests in eastern North America*. Toronto, ON, Canada: Ontario Ministry of Natural Resources.
- Wang, T., Hamann, A., Spittlehouse, D., and Carroll, C. 2016. “Locally downscaled and spatially customizable climate data for historical and future periods for North America.” *PLOS One*, Vol. 11(No. 6): p. e0156720. doi:10.1371/journal.pone.0156720.
- White, J.C., Saarinen, N., Kankare, V., Wulder, M.A., Hermosilla, T., Coops, N.C., Pickell, P.D., Holopainen, M., Hyyppä, J., and Vastaranta, M. 2018. “Confirmation of post-harvest spectral recovery from Landsat time series using measures of forest cover and height derived from airborne laser scanning data.” *Remote Sensing of Environment*, Vol. 216: pp. 262–275. doi:10.1016/j.rse.2018.07.004.
- White, J.C., Wulder, M.A., Hobart, G.W., Luther, J.E., Hermosilla, T., Griffiths, P., Coops, N.C., et al. 2014. “Pixel-based image compositing for large-area dense time series applications and science.” *Canadian Journal of Remote Sensing*, Vol. 40(No. 3): pp. 192–212. doi:10.1080/07038992.2014.945827.
- Wilson, E.H., and Sader, S.A. 2002. “Detection of forest harvest type using multiple dates of Landsat TM imagery.” *Remote Sensing of Environment*, Vol. 80(No. 3): pp. 385–396. doi:10.1016/S0034-4257(01)00318-2.
- Wolf, A.T., Parker, L., Fewless, G., Corio, K., Sundance, J., Howe, R., and Gentry, H. 2008. “Impacts of summer versus winter logging on understory vegetation in the Chequamegon-Nicolet National Forest.” *Forest Ecology and Management*, Vol. 254(No. 1): pp. 35–45. doi:10.1016/j.foreco.2007.07.024.
- Woods, K.D. 2000. “Dynamics in late-successional hemlock–hardwood forests over three decades.” *Ecology*, Vol. 81(No. 1): pp. 110–126. doi:10.1890/0012-9658(2000)081[0110:DILSHH]2.0.CO;2.
- Woods, K.D., and Kern, C.C. 2022. “Intermediate disturbances drive long-term fluctuation in old-growth forest biomass: an 84-yr temperate forest record.” *Ecosphere*, Vol. 13(No. 1): p. e03871. doi:10.1002/ecs2.3871.
- Wulder, M.A., Roy, D.P., Radeloff, V.C., Loveland, T.R., Anderson, M.C., Johnson, D.M., Healey, S., et al. 2022. “Fifty years of Landsat science and impacts.” *Remote Sensing of Environment*, Vol. 280: pp. 113195. doi:10.1016/j.rse.2022.113195.
- Yin, G., Verger, A., Descals, A., Filella, I., and Peñuelas, J. 2022. “A broadband green-red vegetation index for monitoring gross primary production phenology.” *Journal of Remote Sensing, Vol*, Vol. 2022: pp. 1–10. doi:10.34133/2022/9764982.
- Zarnovican, R. 2002. “Impact du verglas de 1998 dans une érablière à bouleau jaune en Estrie : Situation après trois ans.” *The Forestry Chronicle*, Vol. 78(No. 3): pp. 415–421. doi:10.5558/tfc78415-3.